

# Structure of plasma-sprayed oxides in the MgO-Al<sub>2</sub>O<sub>3</sub>-SiO<sub>2</sub> system

H. G. WANG, Y. M. ZHU, H. HERMAN

*Department of Materials Science and Engineering, State University of New York at Stony Brook, Stony Brook, New York 11794-2275, USA*

Cordierite (2MgO · 2Al<sub>2</sub>O<sub>3</sub>-SiO<sub>2</sub>), forsterite (2MgO · SiO<sub>2</sub>) and spinel (MgO · Al<sub>2</sub>O<sub>3</sub>) were rapidly solidified into a thick film through plasma spraying. The crystal structure of the as-sprayed deposits was examined using X-ray diffractometry and transmission electron microscopy, and shows that as-sprayed cordierite is amorphous, as-sprayed spinel is a crystalline phase, and as-sprayed forsterite is a mixture of amorphous and crystalline phases. Moreover, transmission electron microscopy reveals uniform amorphous cordierite, a nonuniform grain-size distribution of crystalline spinel and a twinned texture of as-sprayed forsterite.

## 1. Introduction

Plasma-spray deposition is used industrially to form protective coatings on a wide range of metals and ceramics. In this technique, an electric arc forms a stable plasma flame into which is injected feedstock powder. The powder is rapidly melted and accelerated to the order of sonic velocities and greater [1]. The molten particles impact on to a substrate where rapid solidification occurs and a deposit (in the realm of a "thick film") is formed greater than 25 μm thick. Such deposits show microscopic features indicative of those obtained in other rapid solidification processes [2-4]. In fact, for plasma spraying, the cooling rates are reported to be of the order of 10<sup>6</sup> K sec<sup>-1</sup> by calculating heat transfer between a plasma-jet-sprayed droplet and a highly conducting metal surface [2, 3].

Cooling rate plays an important role in determining microstructure of the as-sprayed deposit [3]. This is clear evidence that the higher the cooling rate, the more metastable will be the obtained deposit. For example, in plasma spraying of alumina, fine particles yield greater proportions of metastable gamma phase than do large particles [4]. It should be noted that fine particles are thought to solidify at higher rates than larger diameter particles (*vis-à-vis*, 20 compared to 40 μm).

Physical and mechanical properties are frequently influenced by microstructure of sprayed oxides. For instance, the thermal expansion coefficient and fracture stress of the plasma-sprayed amorphous cordierite are quite different from those of the hexagonal crystalline structure [5]. The MgO-Al<sub>2</sub>O<sub>3</sub>-SiO<sub>2</sub> system is particularly interesting in a number of deposition technologies (high-temperature applications, molten metal handling, electron device technology). In order to obtain a desired property, one can control the microstructure of sprayed deposit by adjusting the constituents of the sprayed powders. But little is known of the microstructural-spray process relations. This paper is aimed at such a study. Generally, the

as-sprayed deposit is nonuniform and the identified images are difficult to obtain. In this study, we have used X-ray diffractometry (XRD) and transmission electron microscopy (TEM) to investigate the microstructures of three plasma-sprayed oxides of different compositions.

## 2. Experimental procedure

The powders used in this investigation were fused, cast, comminuted cordierite, forsterite and spinel which were all supplied by Muscle Shoals Minerals (Tuscumbia, Alabama). Figs 1a to c are scanning electron micrographs of the as-received powders of cordierite, forsterite and spinel, respectively. The SEM results show that the shape and particle size of the three oxides have no remarkable difference. The particle-size distribution of the oxides using a sieve technique indicates that about 80 wt % of the particles are in the range 37 to 74 μm. The nominal chemistries of the oxides are given in Table I. Using an auto-

TABLE I Chemistry of oxides

Constituent	Oxides (wt %)		
	Cordierite	Forsterite	Spinel
MgO	17.9	50.1	25.9
Al <sub>2</sub> O <sub>3</sub>	31.2		72.9
SiO <sub>2</sub>	50.2	49.6	
Others	0.7	0.3	1.2

TABLE II Plasma-spraying parameters

Parameters	Oxides		
	Cordierite	Forsterite	Spinel
Primary gas; Ar (SLPM)	30	30	40
Secondary gas; H <sub>2</sub> (SLPM)	12	12	13
Carrier gas; Ar (SLPM)	3.4	3.4	4.0
Current (A)	450	500	550
Voltage (V)	74	74	73
Spray distance (mm)	125	110	110
Spray rate (g min <sup>-1</sup> )	9	10	12



Figure 1 Scanning electron micrographs of oxide powders of (a) cordierite, (b) forsterite and (c) spinel.

mated plasma-spray system (Plasma-Technik AG, Switzerland), the powders were deposited on to an NaCl-coated steel substrate. After spraying, the deposits were removed from the substrate by submersion in water, which dissolved the NaCl layer at the steel-oxide coating interface. The plasma-spray parameters are given in Table II.

X-ray diffractometry was carried out with  $\text{CuK}\alpha$  radiation using an automated Philips Diffractometer operating at 45 kV and 40 mA. The scan rate was  $0.25^\circ \text{ min}^{-1}$ . For the TEM study, all the coatings were mechanically polished down to about  $70 \mu\text{m}$  and then ion-beam thinned at an incident angle of  $12^\circ$  to the surface for 8 to 20 h, followed by deposition of a thin layer of carbon before examination under a Philips CM-12 equipped with a double-tilting goniometer and operated at 120 kV.

### 3. Results and discussion

Fig. 2 shows a broad and diffuse XRD pattern, revealing as-sprayed amorphous cordierite. Fig. 3 indicates that as-sprayed forsterite is amorphous, with crystalline forsterite and enstatite. The strong intensity of diffraction peaks and low background, as shown in Fig. 4, indicate that as-sprayed spinel is well crystallized.

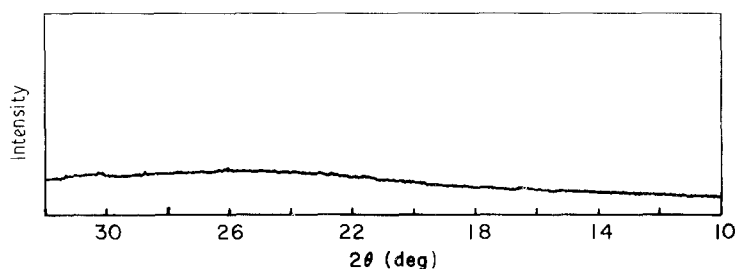


Figure 2 X-ray diffraction pattern of plasma-sprayed cordierite showing amorphicity.

The TEM results, as shown in Figs 5 to 8, are consistent with those obtained from XRD. Fig. 5 is a typical bright-field image of a homogeneous structure of the as-sprayed cordierite. The presence of diffuse haloes in the selected-area diffraction pattern confirms the amorphicity.

Fig. 6 shows the coexistence of the amorphicity and a large crystal of forsterite. This crystal has a plane normal to the  $[210]$  direction. However, it should be noted that the amorphous regions are generally observed to be larger than the crystalline phase. In crystalline forsterite, a twinning texture was observed. Fig. 7a is an enlargement of Fig. 7b, showing a bright-field image of the twinning structure. The observation of the split spots indicated by the arrows in the diffraction pattern (bottom) of crystal A is consistent with the image of the twinning texture. Generally, such twinning structures with the split spots in selected-area diffraction can only be found in some ceramic materials, such as  $\text{YBa}_2\text{Cu}_3\text{O}_{7-x}$  [6]. The twinning is not caused by the translation of atoms, as in most metals, but by the rotation of atoms, which reduces crystal symmetry. In the present case, the twin planes are identified as  $\{101\}$ . The generation of a twinning structure in the oxide is probably due to the release of stress during the rapid solidification process. The selected-area diffraction pattern B-C (upper right of Fig. 7) was taken from an interface of the regions B and C. It shows that diffraction spots of the  $[011]$  diffraction zone are superimposed on the diffuse halo rings and indicates that region C is amorphous and that B is a crystal of forsterite.

A micrograph of as-sprayed spinel, shown in Fig. 8, exhibits a nonuniform grain-size distribution. Very fine grains are distributed in a particle along an interface. A diffraction pattern (A) taken from many small

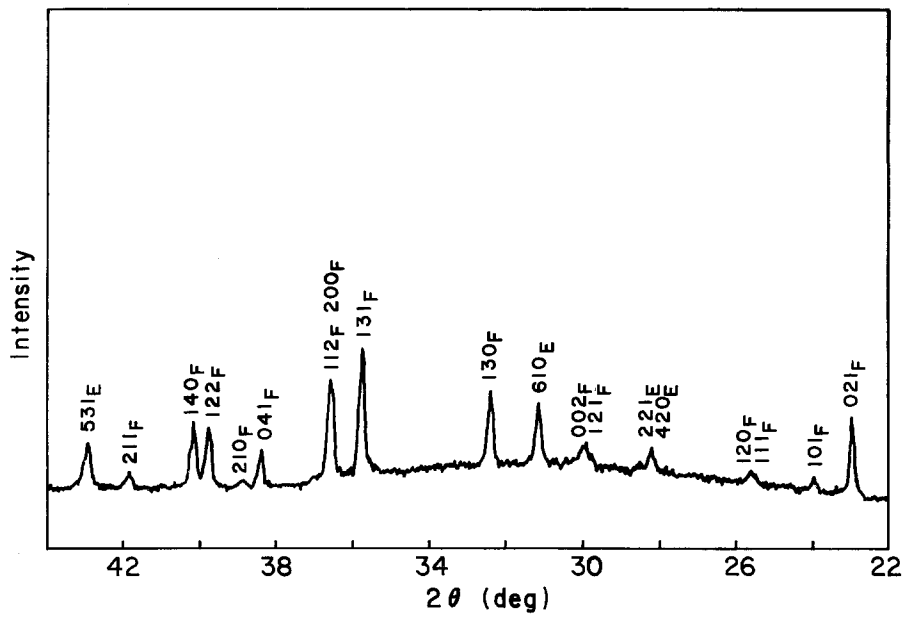


Figure 3 X-ray diffraction pattern of plasma-sprayed forsterite showing amorphicity and crystalline phases of forsterite (F) and enstatite (E).

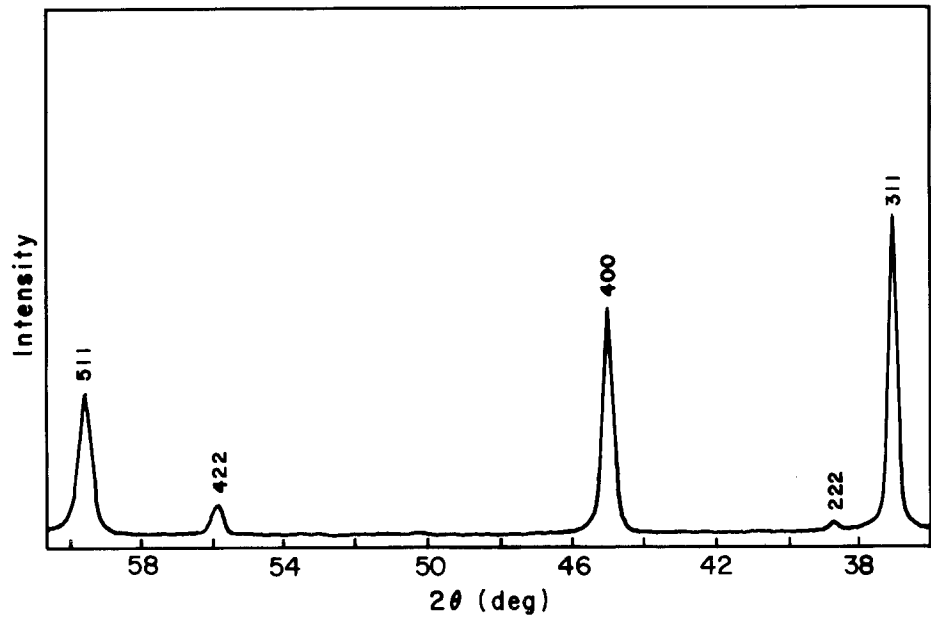


Figure 4 X-ray diffraction pattern of plasma-sprayed spinel showing cubic crystalline phase.

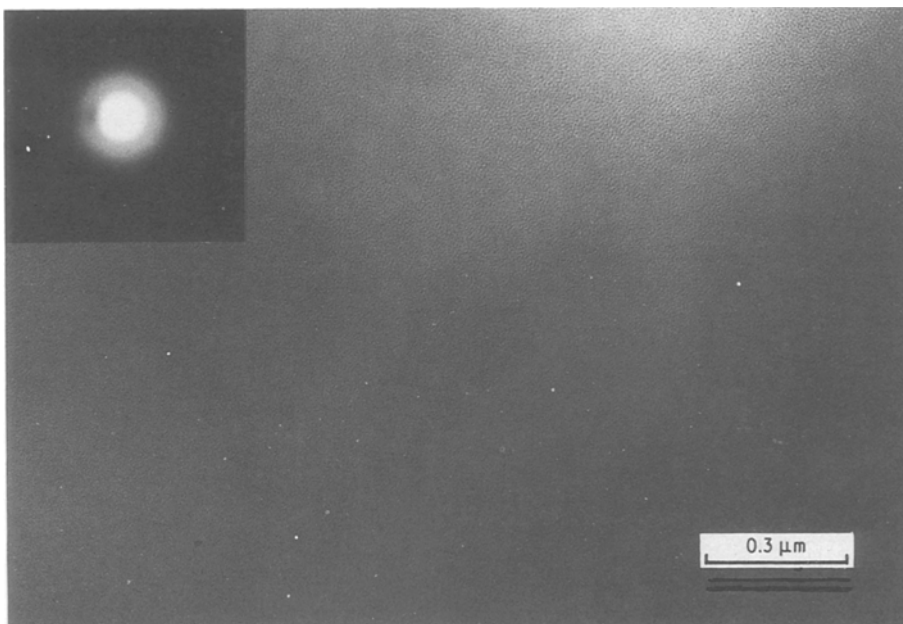


Figure 5 Transmission electron micrograph of plasma-sprayed cordierite showing halo rings in a selected-area diffraction pattern and a low-contrast image.

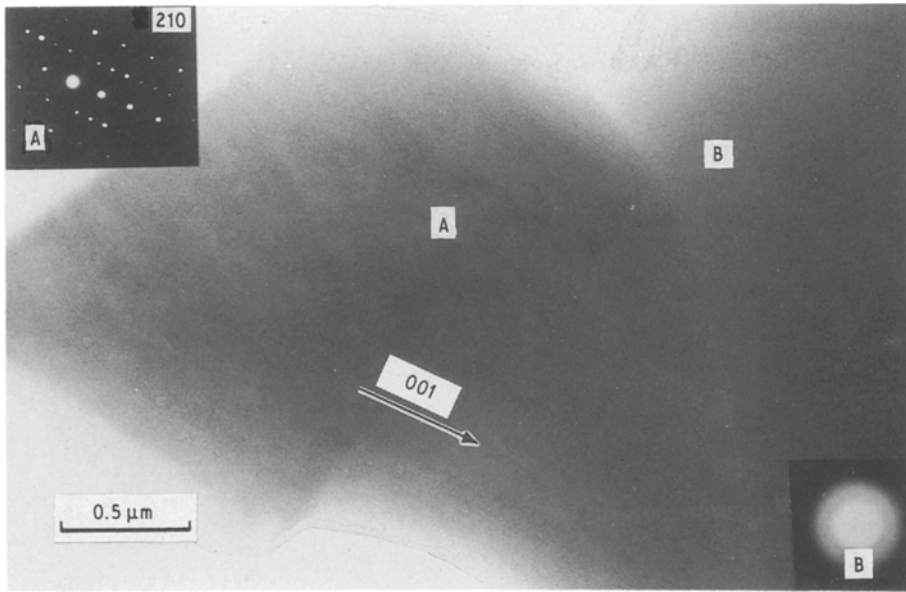


Figure 6 Transmission electron micrograph of plasma-sprayed forsterite showing a crystal (A) in the [2 1 0] zone direction and an amorphous region (B).

grains shows spotty circular rings which are identified as fcc cubic spinel. The grains gradually increase in size towards the interior. Adjacent to the interface are grains some five to ten times larger than those observed at the interface. For example, a strongly diffracting grain, B, is elongated along the [2 0 0] direction. The nonuniform grain-size distribution may be due to variations in cooling rates in the different regions. The smaller grain size results from increased cooling rate [3].

It is believed that the magnitude of the viscosity at the melting temperature and the rate of increase in viscosity with decrease in temperature below the melting point will have a significant influence on establishing crystallinity in oxide systems [7]. In CaO–MgO–SiO<sub>2</sub> and MgO–Al<sub>2</sub>O<sub>3</sub>–SiO<sub>2</sub> glasses, the viscosity increases with additions of silica [8, 9]. From Table I, the oxides contain 50.2, 49.6 and 0 wt % silica for cordierite, forsterite and spinel, respectively. According to an Arrhenius-type equation, the logarithm of viscosity at the melting point is inversely proportional to the melting temperature of oxides [9].

The melting temperatures are 1471, 1910 and 2135° C for the cordierite, forsterite and spinel, respectively [10]. As a result, amorphicity is obtained for cordierite, a mixture of amorphicity and crystallinity for forsterite and a crystalline phase for spinel, even though the cooling rates are of the same order of magnitude for all three oxides.

#### 4. Conclusions

The crystal structure of plasma-sprayed oxides is determined by the cooling rate of the spraying process and the composition of the material. At the same cooling rate, the crystallinity is increased by decreasing the viscosity at the melting temperature, which is determined by silica content and the melting temperature of the oxide. XRD and TEM studies indicate that as-sprayed cordierite is uniformly amorphous, as-sprayed spinel is crystalline phase, with a non-uniform distribution of grain size, and as-sprayed forsterite is comprised of material which is a mixture of amorphous and crystalline where twinning texture is observed.

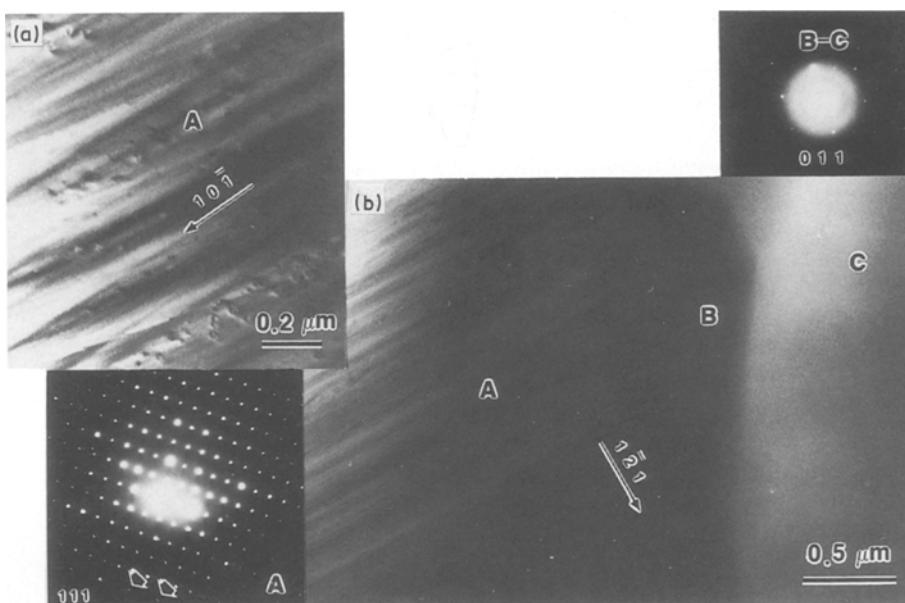


Figure 7 Transmission electron micrograph of plasma-sprayed forsterite showing (a) an enlargement of twin texture (A) with twinning planes in {1 0 1}, (b) the twin structure (A), an adjacent crystal (B) in the [0 1 1] zone direction and amorphous region (C).

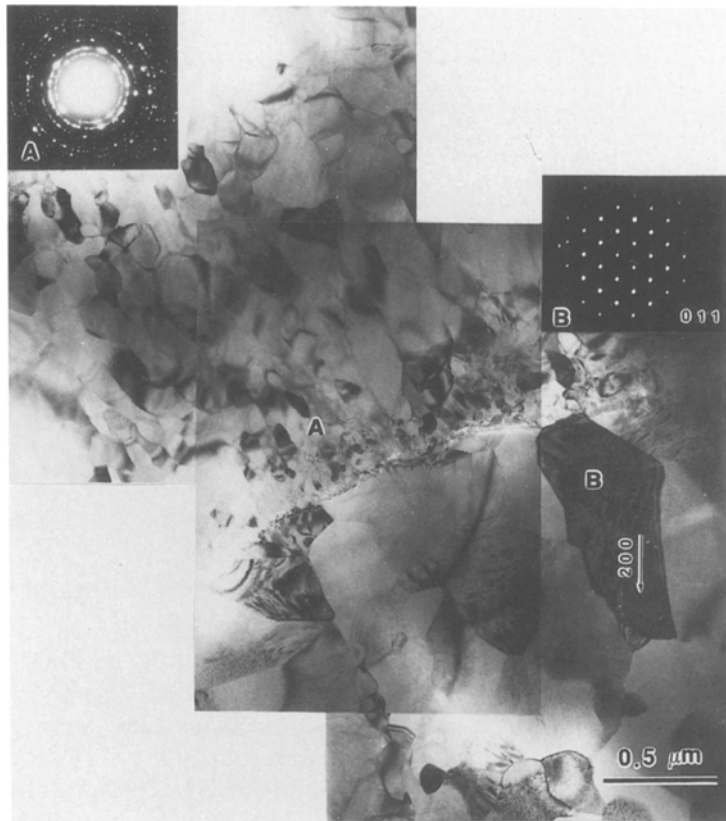


Figure 8 Transmission electron micrograph of plasma-sprayed spinel showing equiaxed small grains in a bright-field image (A) and diffraction rings of fcc cubic structure in a corresponding selected-area diffraction pattern, and an elongated grain (B) along the [200] direction in a large grain area.

## References

1. D. A. GERDEMAN and N. L. HECHT, in "Arc Plasma Technology in Materials Science" (Springer-Verlag, New York, 1972) p. 11.
2. M. MOSS, *Acta Metall.* **16** (1968) 321.
3. S. SAFAI and H. HERMAN, *Treatise Mater. Sci. Technol.* **20** (1981) 183.
4. S. SAFAI, PhD thesis, Materials Science Department, SUNY at Stony Brook, New York (1979).
5. H. G. WANG and H. HERMAN, *Mater. Lett.* **7**(3) (1988) 69.
6. G. VAN TENDELOO and S. AMELINCKX, *J. Electron Microsc. Techn.* **8** (3) (1988) 285.
7. D. R. UHLMANN, *J. Non-Cryst. Solids* **7** (1972) 337.
8. T. LICKO and V. DANEK, *Phys. Chem. Glasses* **27** (1) (1986) 22.
9. E. A. GEISS and S. H. KNICKERBOCKER, *J. Mat. Sci. Lett.* **4** (1985) 835.
10. J. F. LYNCH, C. G. RUDERER and W. H. DUCKWORTH, in "Engineering Properties of Selected Ceramic Materials" (American Ceramic Society, Columbus, Ohio, 1966).

Received 22 September 1988  
and accepted 22 February 1989